

Supersymmetric Z' decays at the LHC

Gennaro Corcella*

INFN, Laboratori Nazionali di Frascati

Via E. Fermi 40, I-00044 Frascati (RM), Italy

E-mail: gennaro.corcella@lnf.infn.it

Searching for Z' bosons, predicted in GUT-inspired $U(1)'$ gauge models and in the Sequential Standard Model, is one of the main challenges of the experiments carried out at the Large Hadron Collider. Such searches have so far focused on high-mass dilepton pairs, assuming that the Z' has only Standard Model decay modes, and have set mass exclusion limits around 2.5-3 TeV. In this talk, I investigate supersymmetric Z' decays at 14 TeV LHC, extending the MSSM in such a way to accommodate extra heavy gauge bosons. In particular, I study Z' decays into pairs of sleptons, charginos and neutralinos, leading to final states with leptons and missing energy, and present results for few reference points of the parameter space, consistent with a SM-like Higgs boson with a mass around 125 GeV. I also discuss the feasibility to search for Dark Matter candidates, by analysing Z' decays into the lightest MSSM neutralinos.

18th International Conference From the Planck Scale to the Electroweak Scale

25-29 May 2015

Ioannina, Greece

*Speaker.

1. Introduction

Heavy neutral gauge bosons Z' are predicted in extensions of the Standard Model (SM), based on $U(1)'$ gauge symmetries, typically inspired by Grand Unification Theories (see, e.g., [1] for a review). Moreover, they are present in the so-called Sequential Standard Model (SSM), wherein Z' and possibly W' bosons have the same couplings to fermions as the Z and W .

The LHC experiments have so far searched for the Z' assuming that it decays into SM channels, focusing on high-mass electron or muon pairs. The absence of this signal has led the ATLAS Collaboration to set the limits $m_{Z'} > 2.90$ TeV in the SSM and $m_{Z'} > 2.51 - 2.62$ TeV in $U(1)'$ models [2], and CMS to set $m_{Z'} > 2.90$ TeV (SSM) and $m_{Z'} > 2.57$ TeV (GUTs) [3]. Hereafter, I study possible decays of the Z' beyond the Standard Model (BSM), taking particular care about supersymmetric final states, within the Minimal Supersymmetric Standard Model (MSSM).

Supersymmetric Z' decays were first considered in [4] and lately reconsidered in [5, 6, 7], in both GUT-inspired and SSM frameworks. Although the SM modes still dominate, the opening of BSM decay channels decreases the branching ratio into dilepton pairs and therefore modifies the LHC exclusion limits. Reference [6], using the same representative point of the MSSM parameter space as in [5], found that the LHC exclusion limits decrease by an amount $\Delta m_{Z'} \simeq 150-300$ GeV, once including supersymmetric decays. However, Refs. [5, 6] chose a reference point which is consistent with the present limits on supersymmetry, but not with the observed Higgs mass, around 125 GeV. Reference [7] extended the investigation in [5] and, by fully including one-loop corrections to the Higgs mass, managed to identify points of the parameter space which are consistent with both supersymmetry searches and Higgs-boson properties.

From the viewpoint of supersymmetry, the production of sparticles in Z' decays has the advantage that their invariant mass is fixed by the heavy boson mass: therefore, if one had to discover a Z' , it would be a cleaner channel to search for supersymmetry, with respect to direct production in $q\bar{q}$ or gg annihilation. Moreover, Z' decays into the lightest neutralinos are interesting processes to search for Dark Matter candidates, since they lead to mono-jet and mono-photon final states (see [8] for a recent study on Dark Matter at the LHC, within the $U(1)'$ extension of the MSSM).

In this talk, I shall highlight the main results of Ref. [7], investigating the feasibility to search for supersymmetry in Z' decays at 14 TeV in $U(1)'$ models.

2. Theoretical framework

$U(1)'$ gauge groups and Z' bosons arise in the framework of a rank-6 Grand Unification group E_6 . The Z'_ψ is associated with $U(1)'_\psi$, coming from the breaking of E_6 into $SO(10)$:

$$E_6 \rightarrow SO(10) \times U(1)'_\psi. \quad (2.1)$$

The subsequent breaking of $SO(10)$ into $SU(5)$ leads to the $U(1)'_\chi$ group and Z'_χ bosons:

$$SO(10) \rightarrow SU(5) \times U(1)'_\chi. \quad (2.2)$$

A generic Z' is then a mixture of Z'_ψ and Z'_χ bosons, with a mixing angle θ :

$$Z'(\theta) = Z'_\psi \cos \theta - Z'_\chi \sin \theta. \quad (2.3)$$

Another scenario, typical of superstring theories, is a direct breaking of E_6 in the SM and a $U(1)'_\eta$ group, leading to a Z'_η boson, with a mixing angle $\theta = \arccos \sqrt{5/8}$:

$$E_6 \rightarrow \text{SM} \times U(1)'_\eta. \quad (2.4)$$

As in [7], in this talk I shall mostly concentrate the analysis on the the Z'_ψ and Z'_η models, as they are the most interesting in the supersymmetric extension of the SM.

In fact, the MSSM gets a few novel features, due to presence of the Z' boson. In addition to the scalar Higgs doublets H_d and H_u , an extra neutral singlet S is necessary to break $U(1)'$ and give mass to the Z' . After electroweak symmetry breaking, the Higgs sector consists of one pseudoscalar A and three scalars h , H and H' , where H' is the new boson, due to the extra $U(1)'$. In the gaugino sector, two more neutralinos are present, associated with the supersymmetric partners of Z' and H' .

Furthermore, as thoroughly debated in [4], the $U(1)'$ group leads to extra D- and F-term contributions to the sfermion masses. In particular, the D-term, depending on the sfermion and Higgs $U(1)'$ charges, can be large and negative, so that even the sfermion squared masses can become negative and thus unphysical (see [5] for a few examples of unphysical configurations).

Hereafter, the Z' mass will always be set to $m_{Z'} = 2$ TeV and the coupling constants of $U(1)'$ and $U(1)_Y$, i.e. g' and g_1 , are assumed to be proportional, as often happens in GUTs:

$$g' = \sqrt{\frac{5}{3}} g_1. \quad (2.5)$$

The supersymmetric parameters $\tan \beta = v_u/v_d$, μ , M_1 , and M' , where M_1 and M' are the soft masses of the gauginos \tilde{B} and \tilde{B}' , are fixed as follows:

$$M_1 = 400 \text{ GeV}, M' = 1 \text{ TeV}, \tan \beta = 30, \mu = 200 \text{ GeV}. \quad (2.6)$$

Given M_1 , the wino mass M_2 can be obtained through $M_2 = (3/5) \cot^2 \theta_W \simeq 827 \text{ GeV}$, θ_W being the Weinberg angle. As for the trilinear couplings $A_{q,\ell}$ of squarks and sleptons with the Higgs in the soft supersymmetric Lagrangian and A_λ , the soft trilinear coupling of the the three Higgs fields (H_u , H_d and S), they are fixed to the same value:

$$A_q = A_\ell = A_\lambda = 4 \text{ TeV}. \quad (2.7)$$

3. Results

In this section I present a few results for the models $U(1)'_\psi$ and $U(1)'_\eta$. In each scenario, a point of the parameter space is chosen, in such a way that at least one decay mode into supersymmetric particles is substantial and leads to an observable signal at the LHC. Besides, in order to suppress QCD backgrounds, particular care will be taken about leptonic final states.

3.1 Phenomenology - $U(1)'_\psi$ model

The Z'_ψ model corresponds to a mixing angle $\theta = 0$ in Eq. (2.3). Following [6], the Z'_ψ mass is set to $m_{Z'} = 2$ TeV, the MSSM parameters as in Eqs. (2.6) and (2.7), whereas the soft sfermion masses at the Z'_ψ mass scale are given by:

$$m_{\tilde{\ell}}^0 = m_{\tilde{\nu}_\ell}^0 = 1.2 \text{ TeV}, m_{\tilde{q}}^0 = 5.5 \text{ TeV}. \quad (3.1)$$

The squark and slepton masses, obtained by summing to the numbers in Eq. (3.1) the D- and F-terms, computed by means of the SARAH [9] and SPheno [10] codes, are quoted in Tables 1 and 2. The notation $q_{1,2}$ and $\ell_{1,2}$ refers to the mass eigenstates, determined from the weak states $q_{L,R}$ and $\ell_{L,R}$, after diagonalizing the mass mixing matrices. Tables 3 and 4 contain the mass spectra of Higgs bosons and gauginos (charginos and neutralinos), respectively. In the Higgs sector, the lightest h has a mass compatible with the SM Higgs, H is roughly as heavy as the Z' , the novel scalar H' , the pseudoscalar A and the charged H^\pm are all above 4 TeV and therefore too heavy to contribute to the decay width of a 2 TeV Z'_ψ . As for the gauginos, with the exception of the heaviest neutralino $\tilde{\chi}_6^0$, they are lighter than the Z'_ψ .

Table 1: Squark masses in GeV the reference point of $U(1)'_\psi$.

$m_{\tilde{d}_1}$	$m_{\tilde{u}_1}$	$m_{\tilde{s}_1}$	$m_{\tilde{c}_1}$	$m_{\tilde{b}_1}$	$m_{\tilde{t}_1}$
5609.8	5609.4	5609.9	5609.5	2321.7	2397.2
$m_{\tilde{d}_2}$	$m_{\tilde{u}_2}$	$m_{\tilde{s}_2}$	$m_{\tilde{c}_2}$	$m_{\tilde{b}_2}$	$m_{\tilde{t}_2}$
5504.9	5508.7	5504.9	5508.7	2119.6	2036.3

Table 2: Masses of charged sleptons ($\ell = e, \mu$) and sneutrinos in the reference point of the $U(1)'_\psi$ model.

$m_{\tilde{\ell}_1}$	$m_{\tilde{\ell}_2}$	$m_{\tilde{\tau}_1}$	$m_{\tilde{\tau}_2}$	$m_{\tilde{\nu}_{\ell,1}}$	$m_{\tilde{\nu}_{\ell,2}}$	$m_{\tilde{\nu}_{\tau,1}}$	$m_{\tilde{\nu}_{\tau,2}}$
1392.4	953.0	1398.9	971.1	1389.8	961.5	1395.9	961.5

Table 3: Masses of neutral and charged Higgs bosons.

m_h	m_H	$m_{H'}$	m_A	m_{H^\pm}
125.0	1989.7	4225.0	4225.0	4335.6

Table 4: Masses of charginos and neutralinos in the reference point of the $U(1)'_\psi$ model.

$m_{\tilde{\chi}_1^+}$	$m_{\tilde{\chi}_2^+}$	$m_{\tilde{\chi}_1^0}$	$m_{\tilde{\chi}_2^0}$	$m_{\tilde{\chi}_3^0}$	$m_{\tilde{\chi}_4^0}$	$m_{\tilde{\chi}_5^0}$	$m_{\tilde{\chi}_6^0}$
204.8	889.1	197.2	210.7	408.8	647.9	889.0	6193.5

The Z'_ψ branching ratios are quoted in Table 5, neglecting rates which are below 0.1%. The overall branching ratio into supersymmetric final states is 28.3%; the rate into chargino pairs $\tilde{\chi}_1^+ \tilde{\chi}_1^-$ accounts for about 10%, while decays into pairs of the lightest neutralinos, i.e. $\tilde{\chi}_1^0 \tilde{\chi}_1^0$, possibly relevant for the searches for Dark Matter, for almost 5%.

Investigating in more detail the $Z'_\psi \rightarrow \tilde{\chi}_1^+ \tilde{\chi}_1^-$ process, subsequent $\tilde{\chi}_1^\pm$ decays may lead to final states with charged leptons and missing energy, as in the following process ($\ell = \mu, e$):

$$pp \rightarrow Z'_\psi \rightarrow \tilde{\chi}_1^+ \tilde{\chi}_1^- \rightarrow (\tilde{\chi}_1^0 \ell^+ \nu_\ell)(\tilde{\chi}_1^0 \ell^- \bar{\nu}_\ell). \quad (3.2)$$

Table 5: Z'_ψ decay rates for $m'_Z = 2$ TeV.

Final State	Z'_ψ Branching ratio (%)
$\tilde{\chi}_1^+ \chi_1^-$	10.2
$\tilde{\chi}_1^0 \tilde{\chi}_1^0$	4.9
$\tilde{\chi}_1^0 \tilde{\chi}_3^0$	0.2
$\tilde{\chi}_2^0 \tilde{\chi}_2^0$	5.1
$\tilde{\chi}_4^0 \tilde{\chi}_4^0$	8.0
hZ	1.4
$W^+ W^-$	2.9
$\sum_i d_i \bar{d}_i$	25.1
$\sum_i u_i \bar{u}_i$	25.0
$\sum_i \nu_i \bar{\nu}_i$	8.3
$\sum_i \ell_i^+ \ell_i^-$	8.3

Table 6: Chargino $\tilde{\chi}_1^+$ decay rates in the reference point of the Z'_ψ model.

Final State	χ_1^+ branching ratio (%)
$\tilde{\chi}_1^0 u \bar{d}$	34.3
$\tilde{\chi}_1^0 u \bar{c}$	1.8
$\tilde{\chi}_1^0 c \bar{d}$	1.6
$\tilde{\chi}_1^0 c \bar{s}$	29.3
$\tilde{\chi}_1^0 e^+ \nu_e$	12.0
$\tilde{\chi}_1^0 \mu^+ \nu_\mu$	12.0
$\tilde{\chi}_1^0 \tau^+ \nu_\tau$	8.9

The decay rates of the charginos are reported in Table 6; the cross section of the process in Eq. (3.2), computed by MadGraph [11], reads: $\sigma(pp \rightarrow Z'_\psi \rightarrow \ell^+ \ell^- + \text{MET}) \simeq 7.9 \times 10^{-4}$ pb at 14 TeV. One may therefore expect about 80 events for a luminosity $\mathcal{L} \simeq 100 \text{ fb}^{-1}$, almost 240 at 300 fb^{-1} .

In the following, I will present some leptonic distributions and compare them with direct decays, $pp \rightarrow Z'_\psi \rightarrow \ell^+ \ell^-$, and direct chargino production, i.e.

$$pp \rightarrow \tilde{\chi}_1^+ \tilde{\chi}_1^- \rightarrow (\tilde{\chi}_1^0 \ell^+ \nu_\ell)(\tilde{\chi}_1^0 \ell^- \bar{\nu}_\ell). \quad (3.3)$$

The cross section of (3.3) is roughly $\sigma \simeq 1.15 \times 10^{-2}$ pb. Furthermore, in (3.2) the $\tilde{\chi}_1^+ \tilde{\chi}_1^-$ invariant mass reproduces $m_{Z'}$, while in (3.3) the charginos do not have this constraint and can be rather soft.

Figure 1 presents the transverse momentum of leptons produced in all three processes, according to MadGraph interfaced to HERWIG [12] for parton showers and hadronization. In direct $Z'_\psi \rightarrow \ell^+ \ell^-$ events, the two leptons get the full initial-state transverse momentum and the p_T spectrum is relevant at high values; in processes (3.2) and (3.3), some (missing) transverse momentum is lent to neutrinos and neutralinos, which significantly decreases the p_T of ℓ^+ and ℓ^- . For direct charginos (3.3) there is no cutoff on the $\chi_1^+ \chi_1^-$ invariant mass and the leptons are quite soft; in $Z'_\psi \rightarrow \chi_1^+ \chi_1^-$, the leptonic p_T is instead higher than in process (3.3).

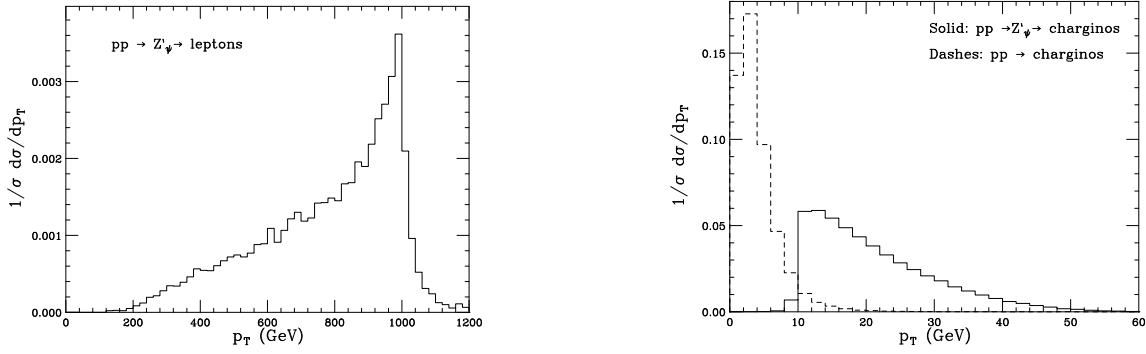


Figure 1: Lepton transverse momentum for the Z'_ψ model at $\sqrt{s} = 14$ TeV and $m_{Z'} = 2$ TeV, for a direct $Z'_\psi \rightarrow \ell^+ \ell^-$ decay (left) and chains initiated by $Z'_\psi \rightarrow \tilde{\chi}_1^+ \tilde{\chi}_1^-$ or direct chargino production processes (right).

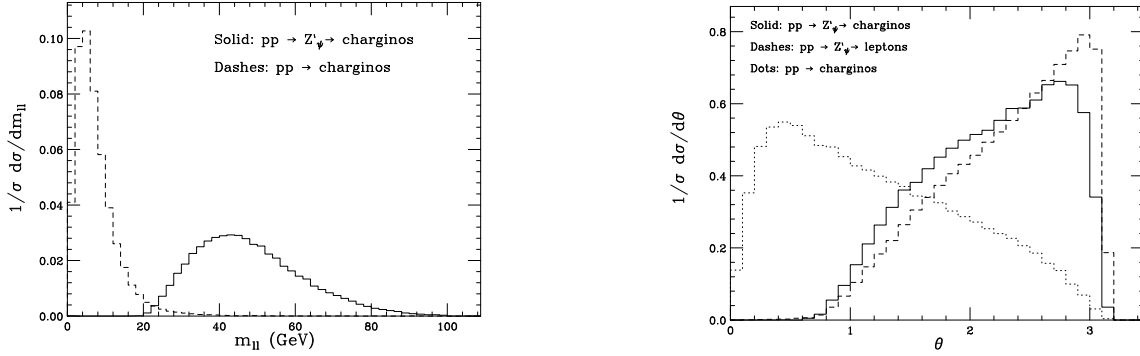


Figure 2: Left: dilepton invariant mass, with ℓ^+ and ℓ^- originated from Z'_ψ decays into charginos and from direct $pp \rightarrow \tilde{\chi}_1^+ \tilde{\chi}_1^-$ events. Right: angle between ℓ^\pm in the laboratory frame, in all three processes.

Fig. 2 presents the $\ell^+ \ell^-$ invariant mass $m_{\ell\ell}$ (left) and the angle θ between the two charged leptons in the laboratory frame (right). In the cascade (3.2), $m_{\ell\ell}$ lies in the range $20 \text{ GeV} < m_{\ell\ell} < 100 \text{ GeV}$ and is maximum at $m_{\ell\ell} \simeq 45 \text{ GeV}$; for direct chargino production, $m_{\ell\ell}$ is peaked about 5 GeV and rapidly decreases. As for the θ spectrum, in Z'_ψ direct leptonic decays it exhibits a maximum about $\theta \simeq 3$, i.e. ℓ^+ and ℓ^- are almost back-to-back; in $Z'_\psi \rightarrow \tilde{\chi}_1^+ \tilde{\chi}_1^-$, the θ distribution is broader and peaked at a lower $\theta \simeq 2.75$; in the chain (3.3), ℓ^+ and ℓ^- are produced at smaller θ .

Figure 3 displays the distributions of the sum of the transverse momenta of ‘invisible’ particles (neutrinos and neutralinos), i.e. the so-called MET (missing transverse energy), and the transverse mass m_T of all final-state particles in Eqs. (3.2) and (3.3). In both processes, the MET spectrum is significant in the low range: in the chain (3.2) it is sharply peaked at $\text{MET} \simeq 20 \text{ GeV}$ and smoothly decreases at larger MET values; for direct chargino production, the MET exhibits an even sharper peak at $\text{MET} \simeq 10 \text{ GeV}$. As for the transverse mass, in (3.3) it is substantial only at small m_T ; in (3.2) it is instead relevant in the range $m_{Z'}/2 < m_T < m_{Z'}$ and peaked just below the Z'_ψ mass threshold, 2 TeV in the present reference point.

Decays into neutralino pairs $\tilde{\chi}_1^0 \tilde{\chi}_1^0$, accounting for almost 5%, are relevant for the searches for Dark Matter candidates and yield a cross section $\sigma(pp \rightarrow Z'_\psi \rightarrow \tilde{\chi}_1^0 \tilde{\chi}_1^0) \simeq 6.4 \times 10^{-3} \text{ pb}$ at 14 TeV LHC. Therefore, about 640 events at $\mathcal{L} = 100 \text{ fb}^{-1}$ and up to almost 2×10^3 at 300 fb^{-1} can be foreseen, with typical signatures given by mono-photon or mono-jet final states. Competing pro-

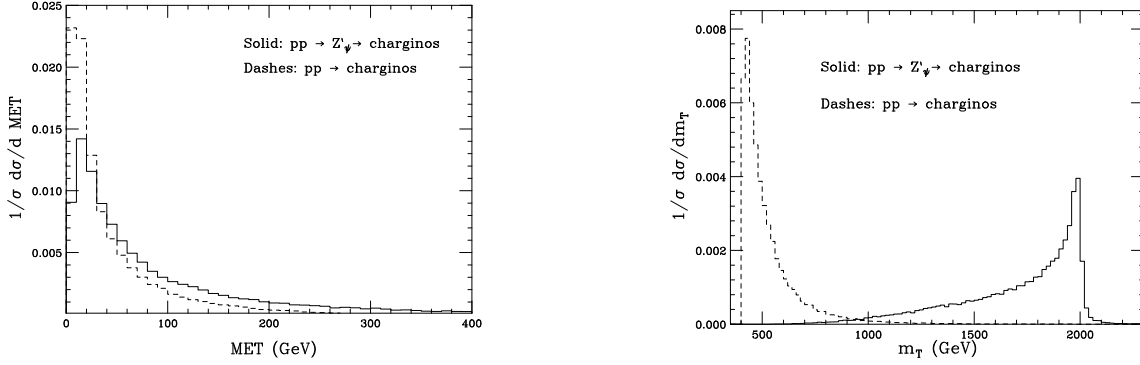


Figure 3: Left: missing transverse energy due to the neutrinos and neutralinos in the cascade initiated by a primary $Z'_\psi \rightarrow \tilde{\chi}_1^+ \tilde{\chi}_1^-$ decay (solid histogram) and for direct chargino production (dashes). Right: transverse mass for the final-state particles (leptons, neutrinos and neutralinos) in the same processes.

cesses are Z'_ψ decays into neutrino pairs, amounting to about $\sigma(pp \rightarrow Z'_\psi \rightarrow \nu\bar{\nu}) \simeq 1.1 \times 10^{-2}$ pb at 14 TeV, with $\mathcal{O}(10^3)$ events at 100 and 300 fb $^{-1}$. Figure 4 displays the total missing transverse energy (MET) spectrum and the contribution due to neutrino and neutralino pairs in Z'_ψ decays; unlike previous distributions, they are normalized to the total LO cross section and not to unity, in such a way to appreciate the discrepancy between the two subprocesses. The shapes of all distributions are roughly the same, but the total number of events at any MET value is higher by about 60% if neutralinos contribute.

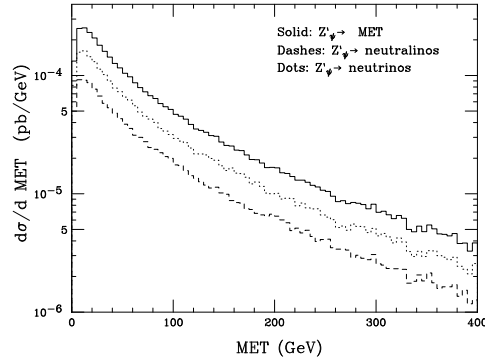


Figure 4: MET spectrum in Z'_ψ decays: plotted are the neutralino (dashes), neutrino (dots) and total (solid) contributions to the missing transverse energy.

3.2 Phenomenology - $U(1)'_\eta$ model

Hereafter, I investigate the $U(1)'_\eta$ model, i.e. $\theta = \arccos \sqrt{5/8}$ in (2.3), for $m_{Z'} = 2$ TeV, MSSM parameters as in Eqs. (2.6) and (2.7) and soft sfermion masses fixed to the following values:

$$m_{\tilde{\ell}}^0 = m_{\tilde{\nu}_\ell}^0 = 1.5 \text{ TeV}, \quad m_{\tilde{q}}^0 = 3 \text{ TeV}. \quad (3.4)$$

After adding D- and F-terms, the masses of squarks and sleptons are those quoted in Tables 7 and 8, whereas Table 9 and 10 contain the masses of Higgs bosons and gauginos, respectively.

Table 7: Squark masses in GeV in the Z'_η model.

$m_{\tilde{d}_1}$	$m_{\tilde{u}_1}$	$m_{\tilde{s}_1}$	$m_{\tilde{c}_1}$	$m_{\tilde{b}_1}$	$m_{\tilde{t}_1}$
3130.8	3129.8	3130.8	3129.8	3130.8	3175.5
$m_{\tilde{d}_2}$	$m_{\tilde{u}_2}$	$m_{\tilde{s}_2}$	$m_{\tilde{c}_2}$	$m_{\tilde{b}_2}$	$m_{\tilde{t}_2}$
3065.9	2863.6	3065.9	2863.6	3065.9	2823.5

Table 8: Slepton masses in the Z'_η scenario.

$m_{\tilde{\ell}_1}$	$m_{\tilde{\ell}_2}$	$m_{\tilde{e}_1}$	$m_{\tilde{e}_2}$	$m_{\tilde{\nu}_{\ell,1}}$	$m_{\tilde{\nu}_{\ell,2}}$	$m_{\tilde{\nu}_{\tau,1}}$	$m_{\tilde{\nu}_{\tau,2}}$
1194.6	1364.5	1208.8	1307.7	1361.8	456.0	1368.0	456.0

Table 9: Higgs bosons in the Z'_η model, with masses expressed in GeV.

m_h	m_H	$m_{H'}$	m_A	m_{H^\pm}
124.9	2004.2	4229.4	4229.4	4230.0

Table 10: Masses in GeV of charginos and neutralinos in the Z'_η model.

$m_{\tilde{\chi}_1^\pm}$	$m_{\tilde{\chi}_2^\pm}$	$m_{\tilde{\chi}_1^0}$	$m_{\tilde{\chi}_2^0}$	$m_{\tilde{\chi}_3^0}$	$m_{\tilde{\chi}_4^0}$	$m_{\tilde{\chi}_5^0}$	$m_{\tilde{\chi}_6^0}$
206.5	882.4	199.3	212.5	408.2	882.3	1562.8	2569.2

Table 11 presents the branching ratios of the Z'_η : within supersymmetry, sneutrino pairs $\tilde{\nu}_2 \tilde{\nu}_2^*$ exhibit the highest rate, slightly below 10%. It is therefore worthwhile investigating the cascade:

$$pp \rightarrow Z'_\eta \rightarrow \tilde{\nu}_2 \tilde{\nu}_2^* \rightarrow (\tilde{\chi}_2^0 \nu_2)(\tilde{\chi}_2^0 \bar{\nu}_2) \rightarrow (\ell^+ \ell^- \tilde{\chi}_1^0 \nu_2)(\ell^+ \ell^- \tilde{\chi}_1^0 \bar{\nu}_2). \quad (3.5)$$

The branching ratios of sneutrinos and neutralinos are given in Tables 12 and 13. The cross section of the cascade (3.5) is $\sigma(pp \rightarrow Z'_\eta \rightarrow 4\ell + \text{MET}) \simeq 1.90 \times 10^{-4}$ pb [7].

In Fig. 5 the transverse momenta of ℓ^\pm in direct decays $Z'_\eta \rightarrow \ell^+ \ell^-$ and of the softest and hardest lepton in the decay chain (3.5) are plotted. In the cascade, the hardest lepton has a broad spectrum, relevant in the $10 \text{ GeV} < p_T < 50 \text{ GeV}$ range, whereas the p_T of the softest ℓ^\pm is a narrow distribution, substantial only for $8 \text{ GeV} < p_T < 20 \text{ GeV}$; the spectrum in the direct production $Z'_\eta \rightarrow \ell^+ \ell^-$ is roughly the same as in the Z'_ψ case.

Figure 6 presents the spectrum of the missing transverse energy and of the transverse mass of the final state (3.5): the MET distribution is similar to the Z'_ψ one; the transverse mass is relevant in the range $m_{Z'}/2 < m_T < m_{Z'}$ and is overall a broader and smoother distribution.

Table 11: Z'_η decay rates in the MSSM reference point for a mass $m_{Z'} = 2$ TeV.

Final State	Z'_η Branching ratio (%)
$\tilde{\chi}_1^+ \chi_1^-$	5.6
$\tilde{\chi}_1^0 \tilde{\chi}_1^0$	1.9
$\tilde{\chi}_2^0 \tilde{\chi}_2^0$	2.1
$\tilde{\chi}_1^0 \tilde{\chi}_2^0$	1.5
$\sum_\ell \tilde{\nu}_{\ell,2} \tilde{\nu}_{\ell,2}^*$	9.4
hZ	1.5
$W^+ W^-$	3.0
$\sum_i d_i \bar{d}_i$	16.1
$\sum_i u_i \bar{u}_i$	25.5
$\sum_i \nu_i \bar{\nu}_i$	27.8
$\sum_i \ell_i^+ \ell_i^-$	5.3

Table 12: Sneutrino $\tilde{\nu}_2$ branching ratios, in the representative point of the Z'_η model.

Final state	$\tilde{\nu}_2$ branching ratio (%)
$\tilde{\chi}_1^0 \nu_2$	4.0
$\tilde{\chi}_2^0 \nu_2$	37.3
$\tilde{\chi}_3^0 \nu_2$	58.7

Table 13: Decay rates for the lighter neutralino $\tilde{\chi}_2^0$.

Final State	$\tilde{\chi}_2^0$ Branching ratio (%)
$\sum_i \tilde{\chi}_1^0 q_i \bar{q}_i$	63.3
$\sum_i \tilde{\chi}_1^0 \ell_i^+ \ell_i^-$	13.4
$\sum_i \tilde{\chi}_1^0 \nu_i \bar{\nu}_i$	20.6

4. Conclusions

I investigated supersymmetric Z' decays at the LHC, for $\sqrt{s} = 14$ TeV, in GUT-inspired $U(1)'_\psi$ and $U(1)'_\eta$ gauge models. The analysis was carried out for few reference points of the MSSM, extended to account for the new $U(1)'$ symmetry, and consistent with a 125 GeV Higgs boson. Both Z'_ψ and Z'_η models yield substantial supersymmetric event rates in the 14 TeV run of the LHC: Z' decays into chargino, sneutrino or neutralino pairs lead to final states with leptons and missing energy, which can be discriminated from $Z' \rightarrow \ell^+ \ell^-$ processes and from direct sparticle production. Once data on high-mass leptons at 14 TeV are available, it will be interesting comparing them with the theory predictions, as done in [6] at 8 TeV, and possibly determine the exclusion limits accounting for supersymmetry. Nevertheless, a full analysis should compare such signals with the backgrounds due to SM, other supersymmetric processes and non-supersymmetric Z' decays, and account for the detector simulation. The inclusion of background and detector effects is in progress.

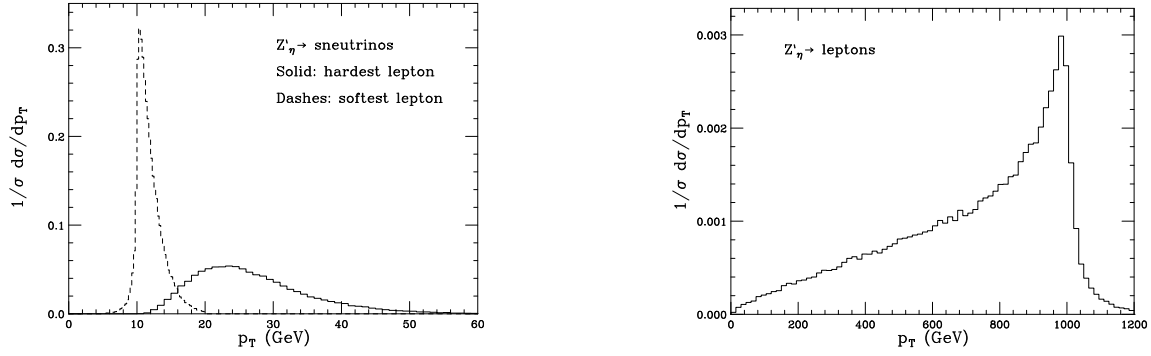


Figure 5: Left: Transverse momentum of the hardest (solid) and softest (dashes) lepton in the cascade initiated by a primary decay into sneutrinos. Right: Lepton transverse momentum in $Z'_\eta \rightarrow \ell^+ \ell^-$ processes.

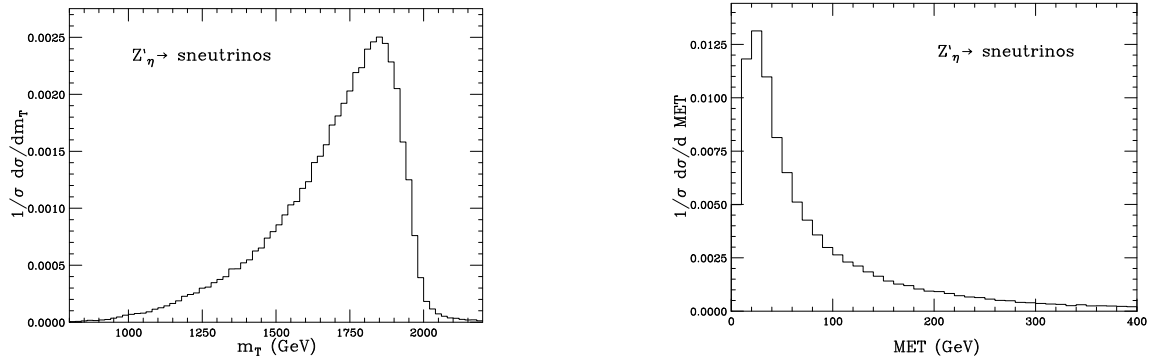


Figure 6: Left: transverse mass of final states initiated by a decay of the Z'_η into sneutrino pairs and leading to a final state with four leptons and MET. Right: missing transverse energy due to neutrinos and neutralinos.

References

- [1] P. Langacker, Rev. Mod. Phys. 81 (2009) 1199.
- [2] ATLAS Collaboration, Phys. Rev. D90 (2014) 052005.
- [3] CMS Collaboration, JHEP 1504 (2015) 025.
- [4] T. Gherghetta, T.A. Kaeding, and G.L. Kane, Phys. Rev. D57 (1998) 3178.
- [5] G. Corcella and S. Gentile, Nucl. Phys. B866 (2013) 293; Erratum-ibid. B868 (2013) 554.
- [6] G. Corcella, EPJ Web Conf. 60 (2013) 18011.
- [7] G. Corcella, Eur. Phys. J. C75 (2015) 264.
- [8] G. Bélanger, J. Da Silva, U. Laa and A. Pukhov, JHEP 1509 (2015) 151.
- [9] F. Staub, Comput. Phys. Commun. 184 (2013) 1792.
- [10] W. Porod and F. Staub, Comput. Phys. Commun. 183 (2012) 2458.
- [11] J. Alwall, M. Herquet, F. Maltoni, O. Mattelaer, T. Stelzer, JHEP 1106 (2011) 128.
- [12] G. Corcella et al, JHEP 0101 (2001) 010.